Turk J Chem
34 (2010) , 639 – 650.

doi:10.3906/kim-0912-379

Synthesis and characterization of gold nanoparticles supported on zinc oxide via the deposition-precipitation method

Hanani YAZID[1], Rohana ADNAN[1,*], Shafida Abdul HAMID[2], Muhammad Akhyar FARRUKH[1,3]

[1] *School of Chemical Sciences, Universiti Sains Malaysia, 11800 Penang-MALAYSIA*
e-mail: r_adnan@usm.my

[2] *Department of Biotechnology, Kulliyyah of Science, International Islamic University Malaysia, 25200 Kuantan, Pahang-MALAYSIA*

[3] *Permanent address: Department of Chemistry, GC University Lahore, PAKISTAN*

Received 16.12.2009

Gold nanoparticles supported on zinc oxide nanoparticles were synthesized at several pH levels via the deposition-precipitation (DP) method. The effects of pH on gold loading, particle size, and particle size distribution on the support were studied at the iso-electric point (IEP) as well as below and above the IEP of ZnO. The addition of the support significantly changed the pH of the solution. The effects of adjusting the pH before and after the addition of the support into the gold chloride solution were also investigated. Gold particles with diameters of less than 5 nm were obtained. The results revealed that gold loading depends on the pH, while gold particle size and distribution are independent of pH adjustment. Structural and elemental characterizations of the gold nanorods were carried out using X-ray diffraction (XRD), transmission electron microscopy (TEM), scanning electron microscopy (SEM), energy-dispersive X-rays (EDX), atomic absorption spectrometry (AAS), and ultraviolet-visible spectrophotometry (UV-Vis).

Key Words: Au nanoparticles, ZnO nanorods, deposition-precipitation, electron microscopy, X-ray diffraction

Introduction

Gold (Au) metal in its bulk form is inert for most chemical reactions. Surprisingly, when gold is synthesized as nano-sized particles, its chemistry drastically changes. It obtains a remarkable ability to catalyze oxidation

*Corresponding author

reactions at low temperatures. This breakthrough emerged when Haruta et al. deposited fine gold particles on selected metal oxides.[1] Since then, the synthesis of gold nanoparticles has come to be of great scientific interest due to their various possible applications. Among the pioneer studies are the catalytic activities of Au supported on titania in a CO oxidation reaction reported by Goodman et al.[2,3] Gold nanoparticles can be synthesized either by vacuum evaporation or as colloids and are recognized as unsupported gold. Vacuum evaporation involves the deposition of thin films of metals on a substrate by evaporation in a vacuum chamber. Meanwhile, colloidal gold nanoparticles are prepared through the use of various reducing agents that generate gold particles with sizes between 20 and 100 nm.[4] Unlike the colloidal technique, smaller gold nanoparticles with sizes of less than 10 nm can be obtained by depositing gold onto a solid support. In the majority of the reported studies, the main supports used for depositing gold were activated carbon and metal oxides, due to their inert properties and high surface areas.[5−10] According to Schimpf et al.,[11] the morphology of supported gold nanoparticles depends upon the type of support used. Remarkable properties in oxidation and hydrogenation reactions have been reported when well-dispersed gold nanoparticles are deposited on an adequate support.[12] Different methods for the synthesis of supported gold nanoparticles have been reported in the literature to obtain well-dispersed particles with nanometer sizes. Among these methods, the most quoted ones are impregnation,[13] coprecipitation,[13,14] and deposition-precipitation.[13,15,16]

The impregnation method is less preferable as it tends to produce large gold particles.[17] Coprecipitation, however, is often used to prepare supported base metal nanoparticles. Preparation involves the addition of chloroauric acid solution and a metal nitrate to a solution of sodium carbonate.[18−20] The most commonly used procedure to synthesize gold nanoparticles is the deposition-precipitation (DP) method. This technique involves the deposition of gold hydroxide on the surface of the metal oxide support by raising the pH of the gold chloride precursors.[21,22] The deposition-precipitation method has an advantage over other methods because the active component, the gold chloride precursor, remains on the surface of the support and not buried in it. Moreover, chloride ions, which are known to poison the activity of gold nanoparticles in many types of reactions, can be minimized by repetitive washing.[23] In addition, gold particles prepared by DP are associated with small particle sizes with a uniform particle distribution[21] and a closed interaction between the gold particles and the support.[13] Therefore, regardless of the numerous methods developed, DP still seems to be the most efficient method to synthesize highly active gold nanoparticles.[24] Specifically for Au/ZnO, little information about preparation using this method under different conditions has been reported.[25] This paper reports on the preparation of Au/ZnO via the DP method and discusses the effects of pH and its adjustment on the morphology of zinc oxide supported gold nanoparticles.

Experimental

Chemicals

The reagents used were gold(III) chloride trihydrate ($HAuCl_4.3H_2O$) and gold atomic absorption standard solutions, all from Sigma-Aldrich, Switzerland. The zinc nitrate and sodium carbonate were from Merck, Germany. Sodium hydroxide (NaOH), silver nitrate ($AgNO_3$), hydrochloric acid (HCl), and nitric acid (HNO_3) were from R&M Chemicals, UK. All reagents were of analytical grade and were used without further purification.

Preparation of gold nanoparticles supported on ZnO

Preparation of ZnO. Zinc oxide was synthesized according to the method reported by Souza et al.[25] In general, 100 mL of zinc nitrate solution (0.2 M) and 100 mL of sodium carbonate (1.0 M) were prepared. The 2 solutions were mixed abruptly, and the precipitates obtained were washed with distilled water and dried under air at 100 °C for 24 h.

Preparation of Au/ZnO. Gold nanoparticles supported on ZnO (Au/ZnO) were prepared by the deposition-precipitation method with some modifications.[15] Gold(III) chloride trihydrate ($HAuCl_4.3H_2O$) was used as the gold precursor. In a typical preparation, 100 mL of $HAuCl_4$ (4.2×10^{-3} M) solution was heated to 80 °C. The pH was adjusted to the desired value by dropwise addition of 0.5 M NaOH. Approximately 1.00 g of the zinc oxide support was dispersed into the solution. Insertion of the support resulted in a pH change, so the pH was kept constant by dropwise addition of 0.5 M HCl. The suspension was thermostated at 80 °C and stirred vigorously for 2 h. Precipitates were washed several times with distilled water to remove residual sodium and chloride ions as well as the unreacted Au species. The washing was considered complete when no AgCl precipitate was detected when the filtrate was added to a $AgNO_3$ solution. Lastly, the precipitates were gathered by centrifugation and dried at 100 °C overnight. The calcination procedure was carried out at 450 °C under air for 4 h with a gradient temperature of 50 °C min^{-1}. The calcination process was necessary as it allows for the decomposition of gold precursors to their metallic state.[26] Preparations of gold nanoparticles supported on ZnO at different pH values of 7, 9.78, and 11, which were below, at, and above the IEP of ZnO, respectively, were repeated using the same procedure. A pH of 9.78 was achieved by the insertion of ZnO into a gold(III) chloride solution without pH adjustment. However, adjustments to pH 7 and 11 were conducted in 2 ways: (1) two-time adjustment, i.e. before and after the addition of ZnO; and one-time adjustment, i.e. only after the addition of ZnO to the $HAuCl_4$ solution with the pH not maintained before the addition of ZnO.

Characterization techniques

UV-Vis spectrophotometry. An ultraviolet-visible (UV-Vis) spectrophotometer (Lambda 35, Perkin Elmer) with a diffuse reflectance sphere for solid phase samples was used to determine the surface plasmon resonance (SPR) for metallic gold. About 10 mg of the sample was mixed with KBr and placed in a cell holder. The absorbance was recorded in the range of 200-800 nm. KBr was used to reduce the concentration of the sample.

XRD spectroscopy. An X-ray diffraction (XRD) diffractometer (X'Pert Pro X-ray diffraction system, Panalytical) was used to investigate the crystal structure of ZnO and Au/ZnO. The sample was ground and pressed into the sample holder to get a smooth plane surface, and the diffraction pattern was recorded over a 2θ range of 30°-120°. The diffractogram obtained was compared to the standard database of the International Centre for Diffraction Data (ICDD).

TEM microscopy. TEM images were obtained with a Phillip CM12 microscope at 80 kV. The sample was suspended in ethanol and homogenized using a sonicator for 15 min. One drop of unsettled suspension was placed on a copper grid and the solvent was allowed to dry at room temperature. The average diameter of particles was calculated by measuring 100-300 individual particles with SIS Soft Imaging GmbH image analysis software.

SEM microscopy. The morphological features of the particles were studied with a scanning electron

microscope (SEM) with an FESEM 50VP, Leo SUPRA instrument. A minimal amount of sample was placed on carbon tape for SEM analysis. An energy-dispersive X-ray detection instrument (EDX) (Oxford INCA 400) was used to examine the elemental composition of the sample.

Atomic absorption spectrometry. The sample was digested with aqua regia and diluted with distilled deionized water. Aqua regia was prepared by mixing 1 part concentrated HNO_3 with 4 parts concentrated HCl to dissolve the gold. Elemental analysis of the amount of gold (Au^{3+}) in the sample was done using an atomic absorption spectrometer (AAnalyst 200, Perkin Elmer) at a wavelength of 243 nm.[17] The Au loading of the samples was expressed in grams of Au per gram of sample: wt% Au = $[m\mathrm{Au}/(m\mathrm{Au} + m\mathrm{ZnO_2})] \times 100$.[15]

Results and discussion

Preparation of Au/ZnO with two-time adjustment of the pH

The effects of pH variation were studied by preparing the supported gold nanoparticles at 2 different pH values of 7 and 11, i.e. below and above the IEP of the zinc oxide.[25] The pH of the solution was adjusted to the desired point before and after the addition of support to the gold chloride solution.

Synthesis of Au/ZnO at a pH lower than the IEP of ZnO

The UV-Vis spectrum of ZnO nanoparticles displayed one peak below 400 nm (Figure 1a).[27] This peak is attributed to the band gap energy for ZnO due to the jumping of electrons from the valence band to the conduction band of the semiconductor after it absorbs light. The Au/ZnO synthesized at pH 7 with two-time pH adjustments exhibits an additional peak at about 550 nm that is attributed to the surface plasmon resonance (SPR) band of the metallic gold (Au^0) (Figure 1b).[15,28]

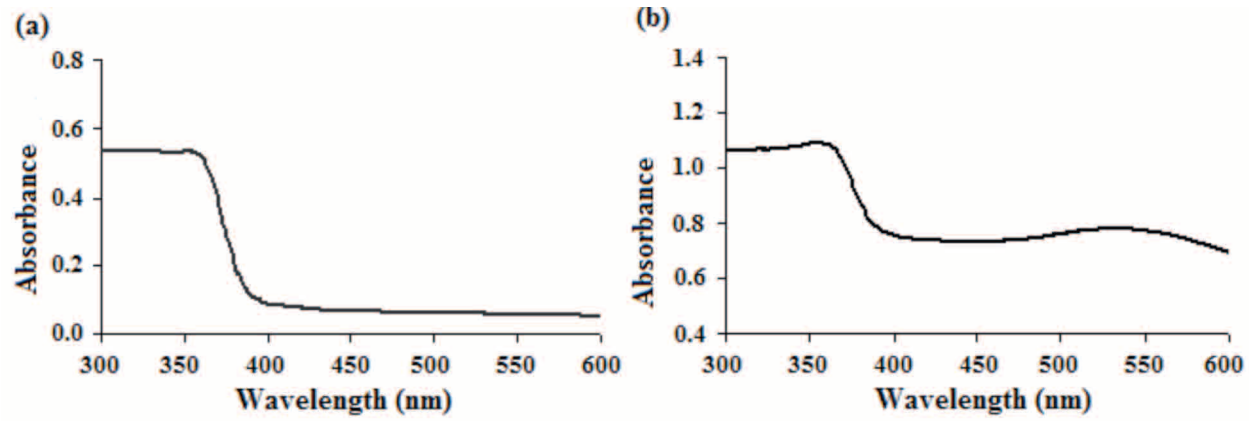

Figure 1. UV-Vis absorption spectra of (a) ZnO and (b) Au/ZnO at pH 7.

The X-ray diffraction (XRD) patterns of Au and Au/ZnO are shown in Figure 2. Figure 2a shows a hexagonal phase (wurtzite structure) of ZnO (JCPDS3-888).[29] The diffraction patterns for gold supported on ZnO (Figure 2b) revealed the diffraction peaks for cubic gold (JCPDS2-1095) at $2\theta = 38°$, $44°$, $82°$, $98°$, $111°$, and $116°$, which correspond to the crystal planes of (1 1 1), (2 0 0), (2 2 2), (4 0 0), (3 3 1), and (4 2

0), respectively.[30] X-ray analysis shows the diffraction lines of a typical cubic crystal structure. Sharper ZnO diffraction peaks were observed when the pH was maintained at 7, which can be attributed to an improvement in the crystal alignment of ZnO.

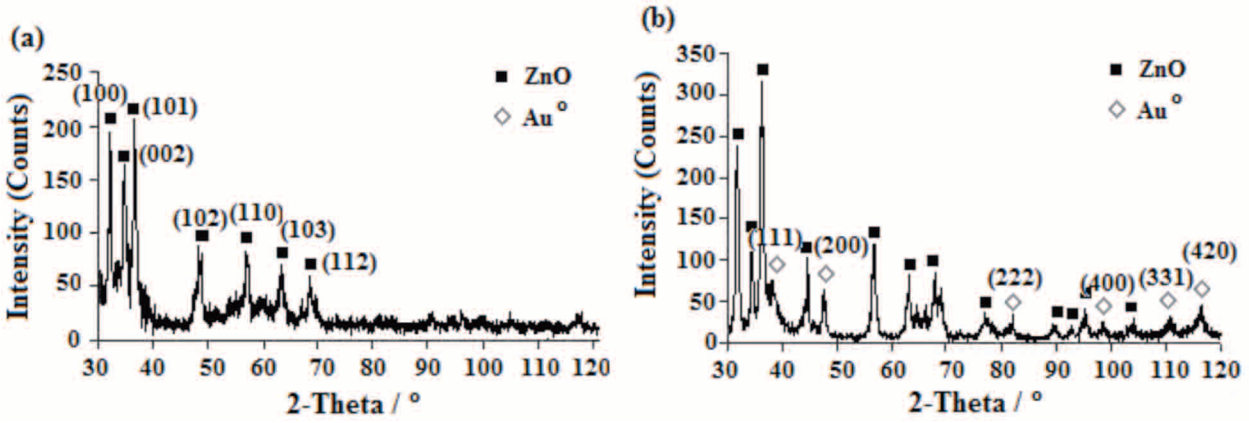

Figure 2. XRD pattern at 2θ: 30°-120° for (a) ZnO and (b) Au/ZnO at pH 7 with adjustments of pH before and after addition of support.

TEM images of ZnO revealed mixed and irregular shapes of nanoparticles (Figure 3a). However, for Au/ZnO at pH 7, distinctive images were observed (Figure 3b), in which gold particles appeared as small dark spherical shapes or dots on the ZnO. The average gold particle size was 4.45 nm. The SEM micrographs display clusters of ZnO rods (Figure 4), while Au/ZnO comprises a mix of shapes of ZnO under the same conditions (Figure 4b), which is in agreement with the TEM images. Shiny dots represent metallic gold in the SEM micrographs.

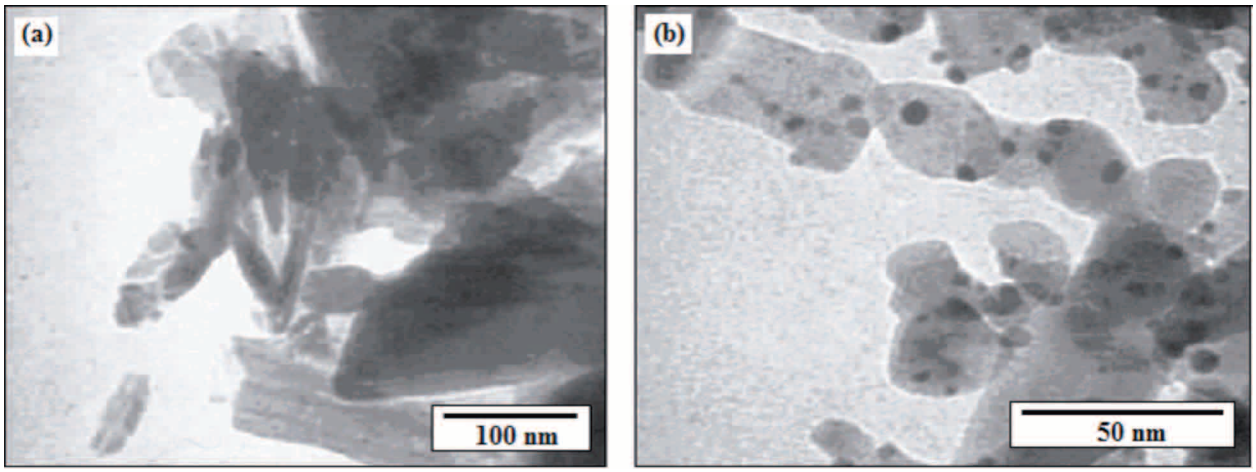

Figure 3. TEM micrographs at pH 7 with adjustments of pH before and after addition of support, (a) ZnO × 145,000 and (b) Au/ZnO × 440,000.

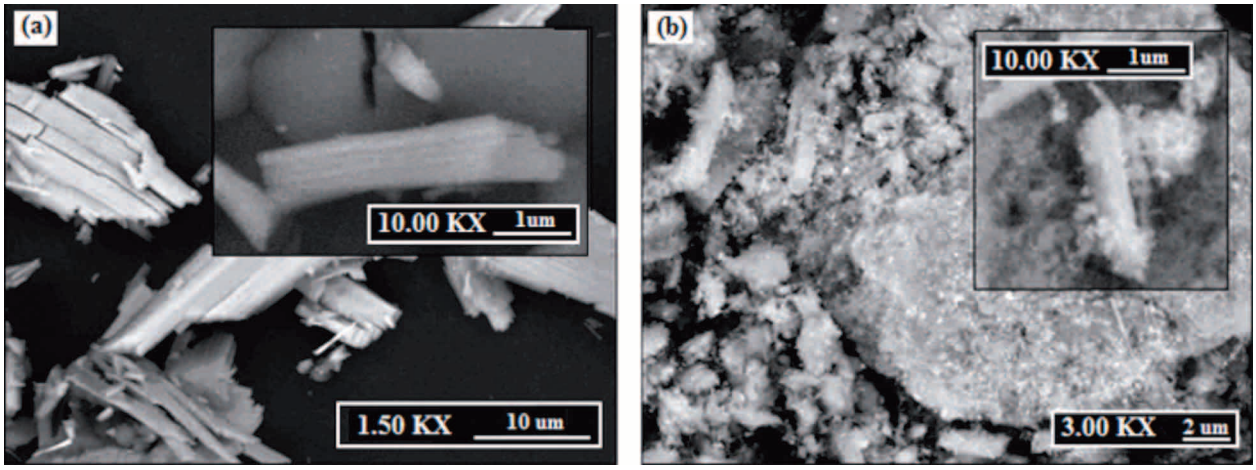

Figure 4. SEM micrographs for (a) ZnO and (b) Au/ZnO at pH 7 with adjustments of pH before and after addition of support.

Synthesis of Au/ZnO at pH higher than the IEP of ZnO

Au/ZnO was synthesized at pH 11 to study the effect of a pH higher than the IEP of ZnO. The XRD patterns of Au/ZnO recorded in the 2θ region of 30°–120° are displayed in Figure 5. The XRD pattern shows 5 peaks to identify the crystalline gold at $2\theta = 44°$, 82°, 98°, 111°, and 116°, which represent the crystal planes of (2 0 0), (2 2 2), (4 0 0), (3 3 1), and (4 2 0), respectively. The disappearance of the diffraction peak at $2\theta = 38°$ indicates that the gold particle size is smaller when fabricated at a pH above the IEP of ZnO. Gold particles were not observed in the TEM images (Figure 6), possibly due to the minimal loading of gold. However, a small amount of gold was detected by SEM-EDX (Figure 7) and AAS analysis (0.198%). The overall results are summarized in the Table. TEM and SEM images revealed that the dominant feature of ZnO is rod-like shape instead of the mix of irregular shapes that occurs when ZnO is prepared at a pH lower than the IEP of ZnO.

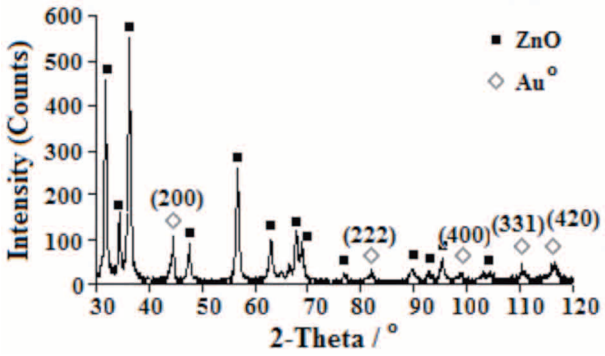

Figure 5. XRD pattern for Au/ZnO at pH 11 with adjustments of pH before and after addition of support.

Table. The gold particle sizes, loadings, and distributions under different conditions.

Samples Au/ZnO	[a]pH required	pH of $HAuCl_4$	[b]First adjustment	Initial pH	pH after addition of support	[c]Second adjustment	Final pH	Au particle size (nm)	Au loadings (wt%)	Au particle distribution (nm)
1	7	1.75	√	7.05	11.74	√	7.28	4.45 ± 1.80	2.653	1-15
2	7	1.75	×	1.75	9.96	√	7.08	4.32 ± 1.26	3.540	1-11
3	11	1.75	√	11.06	13.89	√	11.24	N/A	0.198	-
4	IEP	1.75	×	1.75	9.78	×	9.78	N/A	0.200	-

[a]pH at which synthesis of Au/ZnO was performed

[b]adjustment of pH of gold chloride solution before addition of support

[c]adjustment of pH of gold chloride solution after addition of support

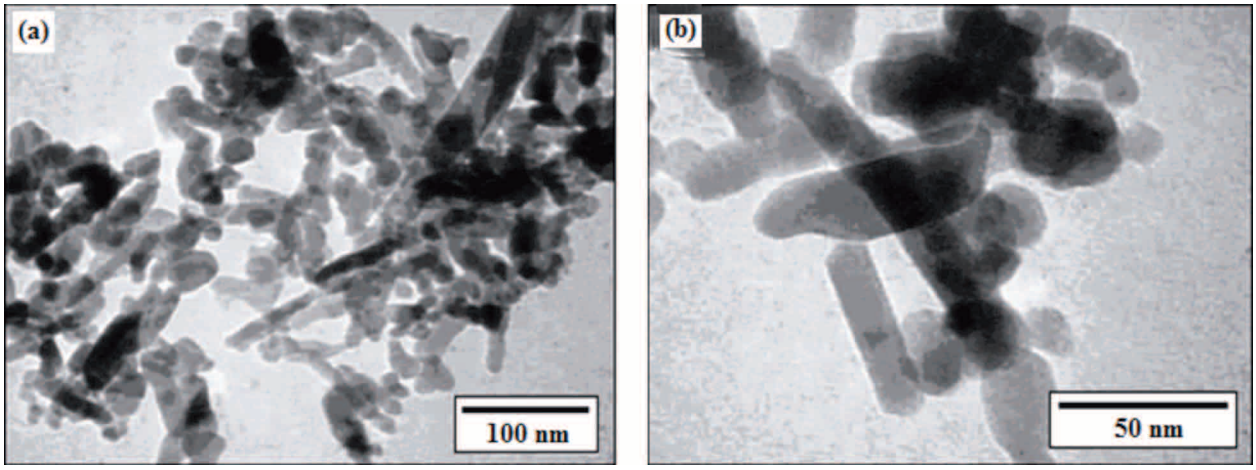

Figure 6. TEM micrographs of Au/ZnO at pH 11 with adjustments of pH before and after addition of support at (a) low magnification of $\times 145{,}000$ and (b) high magnification of $\times 360{,}000$.

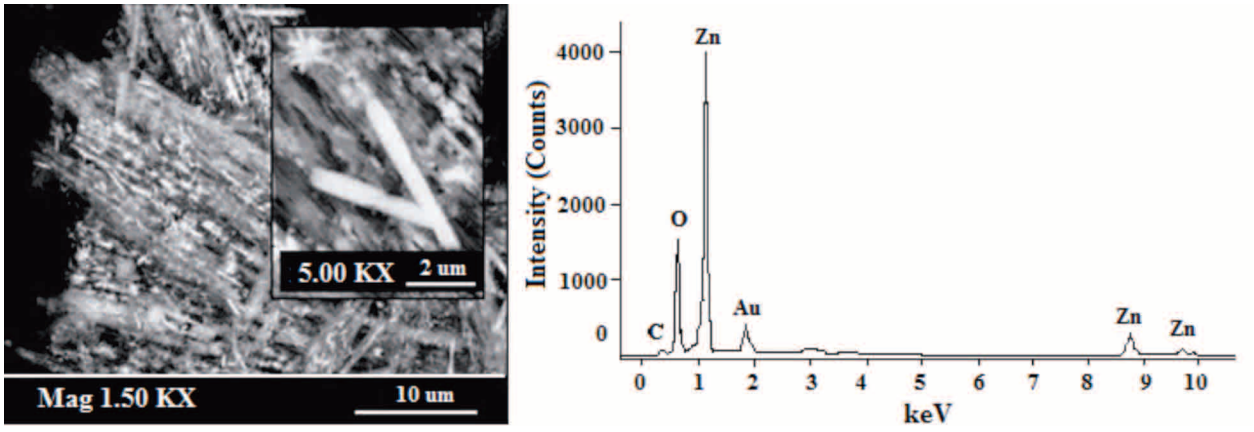

Figure 7. SEM-EDX for Au/ZnO at pH 11 with adjustments of pH before and after addition of support.

Haruta et al.[22,31,32] and Zanella et al.[33] reported that the preparation of supported gold particles at pH < 7 led to the formation of large gold particles. This can be explained by the hydrolysis of the $AuCl_4^-$ precursor in the solution. The hydrolysis is pH dependent and increases when the pH is raised.[34] The author explained that fully hydrolyzed $Au(OH)_4^-$ ions dominate at a pH greater than 8, while below pH 8 the gold precursors contain chloride ions: $[Au(OH)_n Cl_{4-n}]^-$ (n = 1-3). The incorporation of these partially hydrolyzed species on the support surface forms $Au(OH)_3$. These species then change to metallic Au by thermal reduction after the calcination process.[13,21,35] Moreover, the retention of the chloride ions in the solution caused aggregation of the particles into larger clusters during drying and, hence, formed bigger gold particles.

The pH above the IEP leads to minimal gold loadings due to the surface properties of the support.[34] The surface of the metal oxide is covered with a surface hydroxyl species because of its amphoteric character (Zn-OH). Meanwhile, at the IEP of ZnO, both positive and negative charges are balanced. At a pH higher than the IEP, the dominating surface species is $Zn\text{-}O^-$, while at a pH lower than the IEP, $Zn\text{-}OH^+$ dominates.

The surface is positively charged at a pH below the IEP due to the protonation of the surface hydroxyl group. This means that the electrostatic adsorption of the anionic gold chloride precursors occurred as a direct anion exchange, which leads to higher gold loadings. When above the IEP, the surface is negatively charged due to the removal of protons from the surface of Zn-OH. The interaction between the gold chloride precursors and the support therefore involved physical adsorption, which directed the minimal gold loadings.

Influence of pH adjustment

The preparation of gold particles via the DP method generally required the adjustment of the pH before and after the addition of the support. In an attempt to investigate the effect of pH adjustment on the synthesis of gold nanoparticles, 2 additional variations were made: single adjustment of the pH at 7 after insertion of the support, and no adjustment of pH at 9.78, i.e. at the IEP. The effect of one-time adjustment of pH at 11 (after the addition of support) was not studied due to the minimal gold loading (Table).

Figures 8a and 8b display the XRD diffraction peaks for gold at $2\theta = 30°$-$120°$ for gold nanoparticles synthesized at pH values of 9.78 and 7, respectively. The peak at $2\theta = 38°$ was not observed when no adjustment of pH was made due to the small percentage of gold loading and small particle size (Figure 8a). It was confirmed through UV-Visible spectra that particles with sizes of less than 3 nm did not show a defined plasmon band due to quantum-size effects, which led to the formation of quantized energy states.[28] Therefore, the size of the gold particles was found to be smaller than 3 nm.

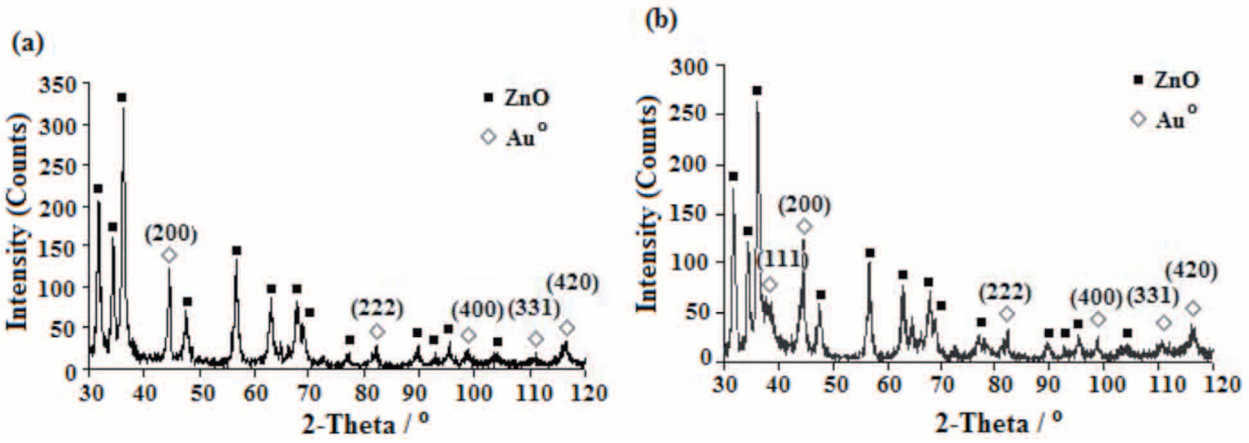

Figure 8. XRD patterns for Au/ZnO (a) at pH 9.78 without adjustment of pH and (b) at pH 7 with adjustment of pH after addition of support.

TEM micrographs at pH 7 show a clear attachment of gold particles onto the ZnO surface, and the ZnO also exhibited a mixture of different shapes of nanoparticles (Figure 9a). TEM images at pH 9.78 showed the absence of gold particles on the surface of the support (Figure 9b). The existence of the gold particles was not detected due to the minimal gold loading (0.200%), as compared to Au/ZnO prepared at other conditions (Table). The average gold particle size determined by TEM was less than 5 nm at pH 7 with one- and two-time adjustment of the pH. Figures 9c and 9d show gold particle distributions at pH 7 with adjustments of pH before and after the addition of support and adjustment of pH after the addition of support only. There was

no significant difference in the average gold particle size. However, gold particles synthesized with one-time adjustment of the pH exhibited narrower particle size distributions as compared to the two-time adjustment. The results are summarized in the Table.

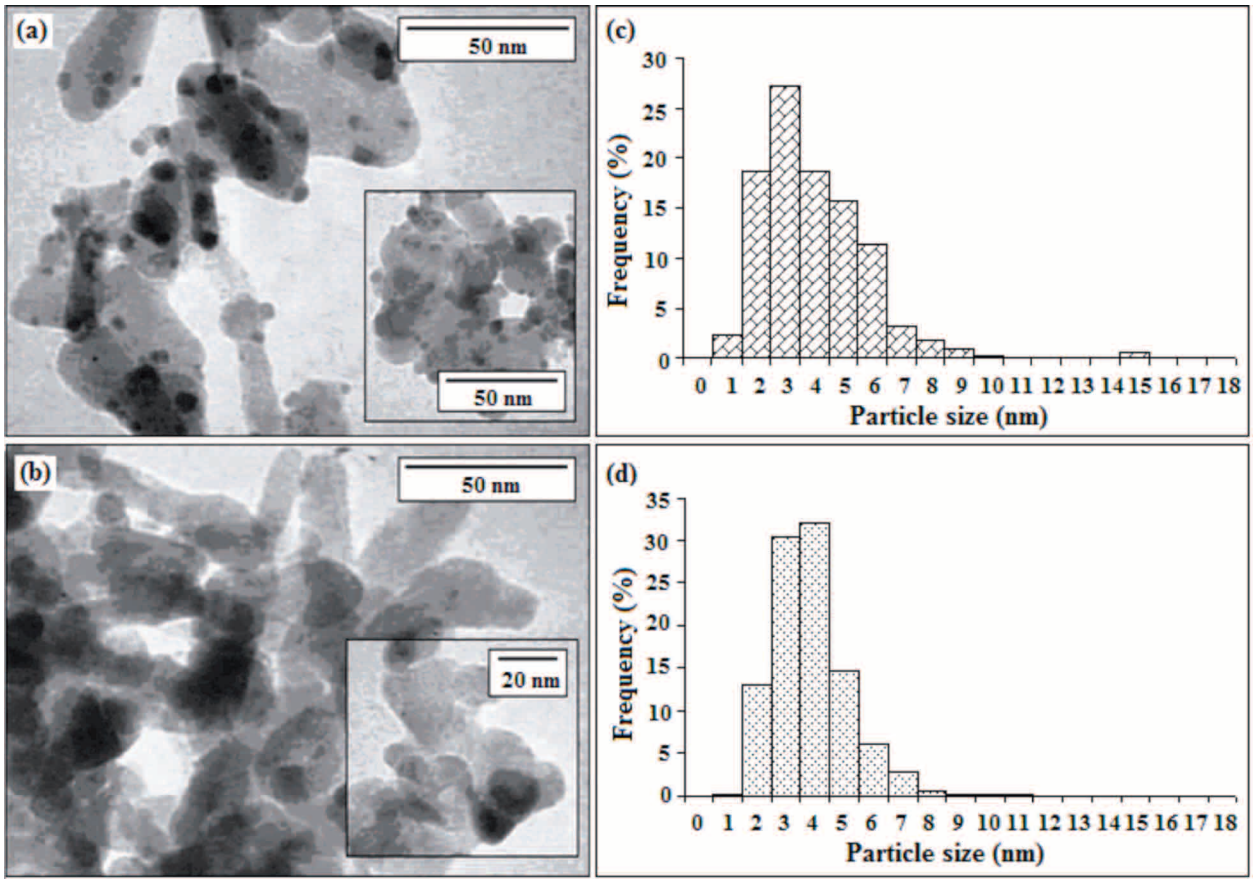

Figure 9. TEM micrographs for Au/ZnO at (a) pH 7 with adjustment of pH after addition of support at × 350,000 (inset × 240,000) and (b) pH 9.78 without adjustment of pH at × 350,000 (inset ×325,000). Distribution of gold particles in Au/ZnO at pH 7 (c) with adjustments of pH before and after addition of support and (d) with adjustment of pH after addition of support.

In this work, gold particle size of less than 5 nm was obtained at pH 7 with one-time adjustment of the pH (after the insertion of support) and with two-time adjustment (before and after the addition of support). The insertion of ZnO into the gold solution directly changed the pH to alkaline conditions. Therefore, similar gold particle size and distribution were achieved because the pH adjustments did not produce different morphological changes to the gold particles or ZnO. The synthesis of Au/ZnO at the IEP resulted in the deposition of gold on ZnO, in which $[AuCl_4]^-$ remained the dominant form.[12] The $[AuCl_4]^-$ complex cannot be exchanged, but it is adsorbed on the surface of ZnO. However, the absence of strong chemical bonding leads to a loss of gold particles during the washing procedures.

Conclusions

Au supported on ZnO nanoparticles via the DP method produced average gold particle size of less than 5 nm with maximal gold loading at pH 7 (lower than the IEP). Minimal gold loadings were found around the IEP of ZnO (pH 9.78) and above the IEP (pH 11). Small gold particle size with a narrow distribution and maximum loading was achieved with a single adjustment of the pH (after the addition of ZnO to the gold precursors, $[AuCl_4]^-$). Rearrangement of irregular shapes of the support (ZnO) to a more organized form was observed at pH 11 in Au/ZnO.

Acknowledgements

Financial support from Universiti Sains Malaysia (USM) under FRGS grant 203/PKIMIA/671046 and PRGS grant 1001/PKIMIA/831002 is gratefully acknowledged. Dr. Muhammad Akhyar Farrukh is a recipient of the TWAS-USM Postdoctoral Fellowship in Research.

References

1. Haruta, M.; Kobayashi, T.; Sano, H.; Yamada, N. *Chem. Lett.* **1987,** *2*, 405-408.
2. Valden, M.; Paka, S.; Lai, X.; Goodman, D. W. *Catal. Lett.* **1998,** *56*, 7-10.
3. Valden, M.; Lai, X.; Goodman, D. W. *Science* **1998,** *281*, 1647-1650.
4. Turkevich, J. *Gold Bull.* **1985,** *18*, 86-91.
5. Ribeiro, N. F. P.; Mendes, F. M. T.; Perez, C. A. C.; Souza, M. M. V. M.; Schmal, M. *Appl. Catal. A: Gen.* **2008,** *347*, 62-71.
6. Schubert, M. M.; Hackenberg, S.; van Veen, A. C.; Muhler, M.; Plzak, V.; Behm, R. J. *J. Catal.* **2001,** *197*, 113-122.
7. Haruta, M. *Catal. Surv. Jpn.* **1997,** *1*, 61-73.
8. Dimitratos, N.; Villa, A.; Bianchi, C. L.; Prati, L.; Makkee, M. *Appl. Catal. A: Gen.* **2006,** *311*, 185-192.
9. Bianchi, C.; Porta, F.; Prati, L.; Rossi, M. *Topics Catal.* **2000,** *13*, 231-236.
10. Milone, C.; Ingoglia, R.; Pistone, A.; Neri, G.; Galvagno, S. *Catal. Lett.* **2003,** *87*, 201-209.
11. Schimpf, S.; Lucas, M.; Mohr, C.; Rodemerck, U.; Brückner, A.; Radnik, J.; Hofmeister, H.; Claus, P. *Catal. Today* **2002,** *72*, 89-94.
12. Ivanova, S.; Pitchon, V.; Petit, C.; Herschbach, H.; Dorsselaer, A. V.; Leize, E. *Appl. Catal. A: Gen.* **2006,** *298*, 203-210.
13. Bond, G. C.; Thompson, D. T. *Catal. Rev. Sci. Eng.* **1999,** *41*, 319-388.
14. Ponec, V.; Bond, G. C. *Catalysis by Metals and Alloys*, Elsevier, Amsterdam, 1996.
15. Zanella, R.; Giorgio, S.; Shin, C. H.; Henry, C. R.; Louis, C. *J. Catal.* **2004,** *222*, 357-367.
16. Moreau, F.; Bond, G. C.; Taylor, A. O. *J. Catal.* **2005,** *231*, 105-114.
17. Lee, S. J.; Gavriilidis, A. *J. Catal.* **2002,** *206*, 305-313.

18. Bailie, J. E.; Hutchings, G. J. *Chem. Commun.* **1999,** 2151-2152.
19. Wang, G. Y.; Zhang, W. X.; Lian, H. L.; Jiang, D. Z.; Wu, T. H. *Appl. Catal. A: Gen.* **2003,** *239*, 1-10.
20. Claus, P.; Hofmeister, H.; Mohr, C. *Gold. Bull.* **2004,** *37*, 181-186.
21. Haruta, M.; Yamada, N.; Kobayashi, T.; Kageyama, H.; Delmon, B.; Genet, M. J. *J. Catal.* **1993,** *144*, 175-180.
22. Haruta, M. *Catal. Today* **1997,** *36*, 153-166.
23. Sakurai, H.; Haruta, M. *Appl. Catal. A: Gen.* **1995,** *127*, 93-105.
24. Li, W. C.; Comotti, M.; Schüth, F. *J. Catal.* **2006,** *237*, 190-196.
25. Souza, K. R.; de Lima, A. F. F.; de Sousa, F. F.; Appel, L. G. *Appl. Catal. A: Gen.* **2008,** *340*, 133-139.
26. Daté, M.; Ichihashi, Y.; Yamashita, T.; Chiorino, A.; Boccuzzi, F.; Haruta, M. *Catal. Today* **2002,** *72*, 89-94.
27. Morales, A. E.; Mora, E. S.; Pal, U. *Rev. Mex. Fis. S* **2007,** *53*, 18-22.
28. Logunov, S. L.; Ahmadi, T. S.; El-Sayed, M. A. *J. Phys. Chem. B* **1997,** *101*, 3713-3719.
29. Mohr, C.; Hofmeister, H.; Radnik, J.; Claus, P. *J. Am. Chem. Soc.* **2003,** *125*, 1905-1911.
30. Aldea, N.; Marginean, P.; Rednic, V.; Pintea, S.; Barz, B.; Gluhoi, A.; Nieuwenhuys, B. E.; Yaning, X.; Aaldea, F.; Neumann, M. *J. Nano. Biostruc.* **2006,** *1*, 71-79.
31. Tsubota, S.; Haruta, M.; Kobayashi, T.; Ueda, A.; Nakahara, Y. In *Preparation of Catalysts V*; Poncelet, G., Ed.; Elsevier Science B. V., Amsterdam, 1991.
32. Haruta, M.; Ueda, A.; Tsubota, S.; Sanchez, R. M. T. *Catal. Today* **1996,** *29*, 443-447.
33. Zanella, R.; Delannoy, L.; Louis, C. *Appl. Catal. A: Gen.* **2005,** *291*, 62-72.
34. Moreau, F.; Bond, G. C. *Catal. Today* **2007,** *122*, 260-265.
35. Kageyama, H.; Kamijo, N.; Kobayashi, T.; Haruta, M. *Physica B* **1989,** *158*, 183-184.